PHYSICAL REVIEW D **84,** 064006 (2011)

Nonstationary regime for quasinormal modes of the charged Vaidya metric

Cecilia Chirenti[1,*] and Alberto Saa[2,†]

[1]*Centro de Matemática, Computação e Cognição, UFABC, 09210-170 Santo André, SP, Brazil*
[2]*Departamento de Matemática Aplicada, UNICAMP, 13083-859 Campinas, SP, Brazil*
(Received 10 May 2011; published 6 September 2011)

We consider nonstationary spherically symmetric n-dimensional charged black holes with varying mass $m(v)$ and/or electric charge $q(v)$, described by generic charged Vaidya metrics with cosmological constant Λ in double-null coordinates and perform a comprehensive numerical analysis of the fundamental quasinormal modes (QNM) for minimally coupled scalar fields. We show that the instantaneous quasinormal frequencies exhibit the same sort of nonstationary behavior reported previously for the four-dimensional uncharged case with $\Lambda = 0$. Such property seems to be very robust, independent of the spacetime dimension and of the metric parameters, provided they be consistent with the existence of an event horizon. The study of time-dependent Reissner-Nordström black holes allows us to go a step further and quantify the deviation of the stationary regime for QNM with respect to charge variations as well. We also look for signatures in the quasinormal frequencies from the creation of a Reissner-Nordström naked spacetime singularity. Even though one should expect the breakdown of our approach in the presence of naked singularities, we show that it is possible, in principle, to obtain some information about the naked singularity from the QNM frequencies, in agreement with the previous results of Ishibashi and Hosoya showing that it would be indeed possible to have regular scattering from naked singularities.

DOI: 10.1103/PhysRevD.84.064006 PACS numbers: 04.30.Nk, 04.40.Nr, 04.70.Bw

I. INTRODUCTION

The quasinormal modes (QNM) analysis is a central tool in the investigation of gravitational perturbations of stars and black holes. (For recent comprehensive reviews of the vast literature on the subject, see [1,2].) The QNM analysis of black holes is particularly relevant due to the possibility of observation of the ringdown signals in gravitational wave detectors such as LISA; see [3] for instance. Besides their relevance for future observations, the QNM can also reveal important information about the structure and behavior of solutions of the Einstein equations. Many generalized solutions have been investigated, including nonasymptotically flat [4–6], charged (see [7] for a comprehensive analysis) and time-dependent ones [8–14]. The AdS/CFT conjecture, in particular, has motivated many QNM analyses of generalized black hole solutions [15]. According to the conjecture, the QNM frequencies carry information about the thermal properties of the associated conformal field theory [1].

The Vaidya metric [16] was originally proposed to describe the spacetime outside a radiating star. It has also been the usual starting point for the study of time-dependent black holes QNM [9–13]. Namely, it corresponds to a time-dependent solution of Einstein equations for a spherically symmetric body immersed in a unidirectional radial null-fluid flow. It has been also widely used in the analysis of spherically symmetric collapse and the formation of naked singularities for many years. (For further references, see [17] and the extensive list of [18]). It is also known that the Vaidya metric can be obtained from the Tolman metric by taking appropriate limits in the self-similar case [19]. This result has shed some light on the nature of the so-called shell-focusing singularities [20], as discussed in detail in [18–23]. The Vaidya metric has also proved to be useful in the study of Hawking radiation and the process of black hole evaporation [24–27], in the stochastic gravity program [28], and in recent numerical relativity investigations [29]. The charged version of the metric is also an usual starting point to the study of many aspects of charged black hole physics and naked singularities [30–34].

The main purpose of the present paper is to consider the QNM of time-dependent backgrounds corresponding to a general Vaidya metric, with special emphasis on nonstationary effects, generalizing and further developing the work done in [11,12]. This kind of QNM analysis is certainly relevant from the physical point of view since, for instance, it is quite natural to expect that a real black hole be affected by processes that can change its mass such as, for instance, mass accretion or even Hawking radiation, which would indeed imply a decreasing mass. Any signal coming from a black hole could, in principle, have some nonstationary component.

As a secondary objective, we show that our numerical setup can be used to investigate the QNM frequencies in the case of a Vaidya metric evolving towards a Reisser-Nordström naked singularity. One should expect the breakdown of our approach in the presence of a naked singularity, of course. However, we show that it is in principle possible to obtain some information about the

*cecilia.chirenti@ufabc.edu.br
†asaa@ime.unicamp.br

singularity from the QNM frequencies, in agreement with the results of Ishibashi and Hosoya [35], who conclude that it is indeed possible to have regular scattering from naked singularities.

This paper has three more sections. In the next one we present the main equations describing the most generic Vaidya metric in double-null coordinates and write the scalar wave equation in a canonical hyperbolic form, specially suitable for the numerical analysis presented in Sec. III. In the last section, we present some concluding remarks.

II. THE SCALAR WAVE EQUATION IN THE VAIDYA SPACETIME

The n-dimensional Vaidya metric was first discussed in [36]. It can be easily cast in n-dimensional radiation coordinates $(v, r, \theta_1, \ldots, \theta_{n-2})$ as done, for instance, in [37]. The n-dimensional charged Vaidya metric in radiation coordinates, obtained originally in [31], reads

$$ds^2 = -\left(1 - \frac{2m(v)}{(n-3)r^{n-3}} + \frac{q^2}{(n-2)(n-3)r^{2(n-3)}}\right)dv^2 + 2cdrdv + r^2 d\Omega_{n-2}^2, \tag{1}$$

where $n > 3$, $c = \pm 1$, and $d\Omega_{n-2}^2$ stands for the metric of the unit $(n-2)$-dimensional sphere, assumed here to be spanned by the angular coordinates $(\theta_1, \theta_2, \ldots, \theta_{n-2})$ in the usual way. For the case of an ingoing radial flow, $c = 1$ and $m(v)$ is a monotonically increasing mass function in the advanced time v, while $c = -1$ corresponds to an outgoing radial flow, with $m(v)$ being in this case a monotonically decreasing mass function in the retarded time v. The constant q corresponds to the total electric charge. In principle, one can also consider time-dependent charges q as done, for instance, in [32]. This situation will of course require the presence of charged null fluids and currents, whose realistic nature we do not address here. We have already reported some preliminary results on QNM for this case in [38].

We will now extend the approach proposed in [39,40] and derive the double-null formulation for the most general Vaidya metric: n-dimensional, in the presence of a cosmological constant, and with varying electric charge. Only the main results are presented. The reader can get more details on the employed semianalytical approach in [39,40] and the references cited therein. We recall that the n-dimensional spherically symmetric line element in double-null coordinates $(u, v, \theta_1, \ldots, \theta_{n-2})$ is given by

$$ds^2 = -2f(u, v)dudv + r^2(u, v)d\Omega_{n-2}^2, \tag{2}$$

where $f(u, v)$ and $r(u, v)$ are nonvanishing smooth functions. The energy-momentum tensor of a unidirectional radial null-fluid in the eikonal approximation in the presence of an electromagnetic field F_{ab} is given by

$$T_{ab} = \frac{1}{8\pi}h(u, v)k_a k_b + \frac{1}{4\pi}\left(F_{ac}F_b{}^c - \frac{1}{4}g_{ab}F_{cd}F^{cd}\right), \tag{3}$$

where k_a is a radial null vector and $h(u, v)$ is a smooth function characterizing the null-fluid radial flow. We will consider here, without loss of generality, the case of a flow along the v direction.

From the Einstein-Maxwell equations with metric (2) and energy-momentum tensor (3) we obtain the following equations for the functions f, h, and r:

$$f = 2Br_{,u}, \tag{4}$$

$$h = -2\left(\frac{n-2}{n-3}\right)\frac{B}{r^{n-2}}\left(m_{,v} - \frac{1}{n-2}\frac{(q^2)_{,v}}{r^{n-3}}\right), \tag{5}$$

$$r_{,v} = -B\left(1 - \frac{2m(v)}{(n-3)r^{n-3}} - \frac{2\Lambda r^2}{(n-2)(n-1)} + \frac{2q^2(v)}{(n-2)(n-3)r^{2(n-3)}}\right), \tag{6}$$

where $B(v)$, $m(v)$, and $q(v)$ are arbitrary integration functions. If we choose $B(v) =$ constant, we can interpret $m(v)$ and $q(v)$ as the mass and charge of the solution, respectively. These two functions must be monotonic and must be chosen in a way that satisfies the null-energy condition [32]. The details of the derivation of Eqs. (4)–(6) and the full analysis of the charged Vaidya metric in duble null coordinates will be presented in another paper currently under preparation.

For our QNM analysis we will consider the evolution of a massless scalar field governed by the Klein-Gordon equation

$$\frac{1}{\sqrt{-g}}(\sqrt{-g}g^{ab}\Psi_{,b})_{,a} = 0, \tag{7}$$

in the background (2). Taking advantage of the spherical symmetry, we decompose the scalar field in terms of higher-dimensional spherical harmonics

$$\Psi = \sum_{\ell,m}\psi(u, v)Y_{\ell m}(\theta_1, \ldots, \theta_{n-2}), \tag{8}$$

for which

$$\nabla_\Omega^2 Y_{\ell m} = -\ell(\ell + n - 3)Y_{\ell m}, \tag{9}$$

where ∇_Ω^2 stands for the Laplacian operator over the $(n-2)$-dimensional unit sphere. Substituting the ansatz (8) in (7), we obtain for the metric (2)

$$\frac{1}{fr^{n-2}}((r^{n-2}\psi_{,v})_{,u} + (r^{n-2}\psi_{,u})_{,v}) + \frac{\ell(\ell+n-3)}{r^2}\psi. \tag{10}$$

Using now the substitution $\psi = r^{-(n-2/2)}\varphi$, we get

$$\varphi_{,uv} + V(u, v)\varphi = 0, \tag{11}$$

where

$$V = \frac{\ell(\ell+n-3)}{2r^2} f - \frac{(n-2)(n-4)}{4r^2} r_{,u} r_{,v} - \frac{(n-2)}{2r} r_{,uv}. \tag{12}$$

The wave Eq. (11) is already written in a canonical hyperbolic form and it will be the starting point for our QNM analysis. Nevertheless, the potential (12) can still be cast in a more convenient way. From Eqs. (4) and (6), we find

$$r_{uv} = -f\left(\frac{m}{r^{n-2}} - \frac{2\Lambda r}{(n-2)(n-1)} - \frac{2q^2}{(n-2)r^{2n-5}}\right), \tag{13}$$

and

$$r_{,u} r_{,v} = -f\left(\frac{1}{2} - \frac{m}{(n-3)r^{n-3}} - \frac{\Lambda r^2}{(n-2)(n-1)} + \frac{q^2}{(n-2)(n-3)r^{2(n-3)}}\right). \tag{14}$$

Now we can finally write the potential $V(u, v)$ as

$$V(u,v) = \frac{f}{2}\left(\frac{\ell(\ell+n-3)}{r^2} + \frac{(n-2)(n-4)}{4r^2} + \frac{(n-2)^2 m(v)}{2(n-3)r^{n-1}} - \frac{n\Lambda}{2(n-1)} - \frac{(3n-8)q^2(v)}{2(n-3)r^{2(n-2)}}\right). \tag{15}$$

The conventions we adopted for the mass, electric charge, and cosmological constant appearing in the potential (15) and used in the derivations of this section are the standard ones employed in the Vaidya metric literature. In particular, our expressions coincide, in the appropriate limits, with the previous results for the $\Lambda = 0$ [31] and for the $q = 0$ [40] cases. However, the commonly employed conventions in the QNM literature are slightly different; see, for instance, [41].

III. NUMERICAL RESULTS

The wave Eq. (11) is already written in a canonical hyperbolic form and it can be numerically integrated by means of a characteristic scheme, i.e., one can evolve $\varphi(u, v)$ in v knowing $\varphi(u, v_0)$. In order to determine $V(u, v)$, one needs to know $f(u, v)$ and $r(u, v)$ and, consequently, Eq. (6) must be solved in each evolution step. Since only $\varphi(u, v)$ is required to determine $\varphi(u, v + dv)$, one can implement the algorithm in an efficient way avoiding unnecessary calculations. We use here the same numerical scheme used in [11,12] to evolve the system and read the QNM frequencies, which allows us to perform an exhaustive numerical analysis with modest computational resources.

All mass functions considered in this work are of the form

$$2m(v) = (m_f + m_i) + (m_f - m_i)\tanh\rho_m(v - v_m), \tag{16}$$

where m_i and m_f stand for the initial and final mass, respectively, and ρ_m controls how fast the change is, with the maximum rate of change at $v = v_m$. We use an analogous expression for the time-dependent electric charge $q(v)$. Our main results do not depend on the exact form of the functions $m(v)$ and $q(v)$. Choices such as (16), however, are very convenient due to their smooth behavior and the "asymptotically static" limits for $v \to \pm\infty$.

For the numerical calculation of the v-evolution, the algorithm requires the evaluation of $\varphi(u, v)$ for all values of u corresponding to the exterior region of the black hole, let us say, for $u_h < u < \infty$, with $u = u_h$ corresponding to the event horizon. Technically, it is easier to control the approach to the regions near the horizon by introducing an appropriated kind of tortoise coordinate U such that the external region $u_h < u < \infty$ will correspond to $-\infty < U < \infty$.

A. Static case: Reissner-Nordström black hole

It is instructive to start by testing our code with the standard Reissner-Nordström (RN) case, for which a vast set of results is available in the literature [7]. The potential (15) for $n = 4$ and $\Lambda = 0$ becomes simply

$$V(u, v) = \frac{f}{2}\left(\frac{\ell(\ell+1)}{r^2} + \frac{2m}{r^3} - \frac{2q^2}{r^4}\right). \tag{17}$$

In order to compare the QNM frequencies obtained from the numerical integration of (11) for the potential (17) with well-known results for the RN black hole, we perform the following change of variables:

$$U = u - \frac{2r_+^2}{r_+ - r_-}\ln\left(-\frac{u}{2} - r_+\right) - \frac{2r_-^2}{r_+ - r_-}\ln\left(-\frac{u}{2} - r_-\right), \tag{18}$$

where

$$r_\pm = m \pm \sqrt{m^2 - q^2}, \tag{19}$$

as usual for the RN black hole. This is necessary in order to guarantee that the QNM frequencies be defined with respect to the same scales. Moreover, the new tortoise coordinate U given by (18) allows a better description of the exterior region of the black hole, notably of the regions very close to the horizon r_+. The numerical grid is, therefore, written in $U \times v$ coordinates, and u is obtained by inverting the definition (18).

A comparison between the numerical results obtained with our code and the values found in the literature is shown in Fig. 1. We observe a very good agreement with the known values for the RN QNM frequencies. This simple example allows us to calibrate all the algorithm parameters in order to attain a preestablished accuracy.

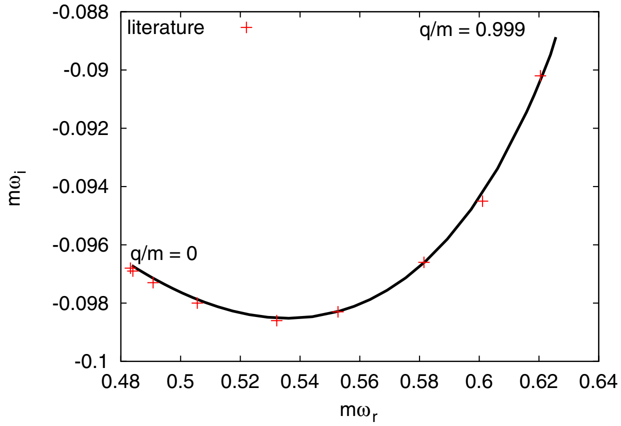

FIG. 1 (color online). Frequencies of the quasinormal modes of a scalar perturbation with $\ell = 2$ obtained for an RN black hole with our code (smooth line) compared with values found in the literature [41,50].

B. Time-dependent case

We perform a comprehensive QNM analysis for the wave Eq. (11) with the potential (15). We are mainly interested in the nonstationary regimes like the one described in [11], corresponding to the case $q = 0$, $n = 4$, and $\Lambda = 0$ in the potential (15). As we show in this section, the stationary and nonstationary regimes for QNM are also present for the general situation corresponding to the potential (15). Moreover, we verify appreciable deviations from the stationary regime whenever $|m''(v)|$ or $|q''(v)|$ is larger than $|\omega_I|$, where ω_I is the imaginary part of the first QNM frequency. This behavior occurs irrespective of the other parameters of the potential (15), provided they be consistent with the existence of a black hole.

The case of an asymptotically flat ($\Lambda = 0$) "time-dependent RN black hole," i.e., an RN black hole with time-dependent mass $m(v)$ and/or charge $q(v)$ functions, is particularly interesting. The determination of the new tortoise variable U equivalent to (18) is quite more involved for this case. The problem here is the definition, and the numerical determination, of the event horizon. (See [40] for a discussion of the implications of this problem in the semianalytical approach used here.)

For our purposes here, the event horizon r_+ is the last null geodesic (up to the machine precision) escaping towards infinity, requiring the full numerical solution of (6) prior to the analysis of the wave Eq. (11). The determination of the real Cauchy horizon r_- is easier since any null geodesic inside the event horizon tends to r_- along the v evolution.

In Fig. 2, we present the time variation for the real and imaginary parts of the QNM of the scalar perturbations with $\ell = 2$ for a four-dimensional RN black hole with time-dependent mass and charge functions. The QNM frequencies change in a similar way with the time variation of the mass or the charge, but they are typically more sensitive to the charge variations.

The results from the lower plot of Fig. 2 can also be seen in Fig. 3, in the $\omega_r \times \omega_i$ plane, where we see how the variation goes from one stationary state to another through a nonstationary trajectory. In the right plot of Fig. 3, we use the minimum value of the variation of ω_i in the nonstationary trajectories of the left plot to quantify the deviation from the stationary trajectory. These values are plotted against ρ, which can be related to a measure of how fast the variations are. We can see that the behavior can be described extremely well by a linear fit at first, deviating from this fit for $\rho \gtrsim 0.1$ (faster variations).

The case of asymptotically extremal ($q_f = m_f$) black holes is specially notable in our approach due to numerical technicalities. Our results for this case are presented in Fig. 4. In the right plot we present a convergence test, essential in this case, with the results obtained for different resolutions, while in the left plot we show how the results depend on the manner in which $q(v) \to m$. We remind the reader here that an extremal RN black hole is, of course, yet a regular black hole and not a naked singularity, and its QNMs are well defined. It is only due to numerical limitations that most works in the literature do not reach this limit.

The left plot of Fig. 4 shows once again that the deviation from the stationary behavior increases as we consider faster variations of the background, which are quantified by ρ. As this deviation becomes smaller, however, it is possible to note a nontrivial trajectory of the complex frequencies in the plane (more easily discernible in the right plot), whose origin is still unclear.

C. Formation of a naked singularity

We can use our formalism and numerical setup to probe the formation of a naked singularity in the spacetime. The idea that it would be possible to have regular scattering from naked singularities is rather old [42]. In fact, as it was first noticed by Gibbons [43], minimally coupled scalar fields have the remarkable property of being regular at the origin of a Reissner-Nordström solution, where the spacetime manifold is irremediably singular. The nonsingular behavior of scalar [44] and other [45] fields around a Reissner-Nordström naked singularity has been investigated since then. Despite being mathematically well posed, the field dynamics near a naked singularity are typically ambiguous from the physical point of view since it is not clear which boundary condition one needs to impose for the field at the singularity.

The main motivation of this part of our investigation is the work of Ishibashi and Hosoya [35], which demonstrated explicitly that it is indeed possible to have unambiguous and regular scattering from naked singularities. After all, the presence of a naked singularity might be less harmful than originally conceived. This has been explored recently in a quantum field theory scenario in the series of papers [46–49].

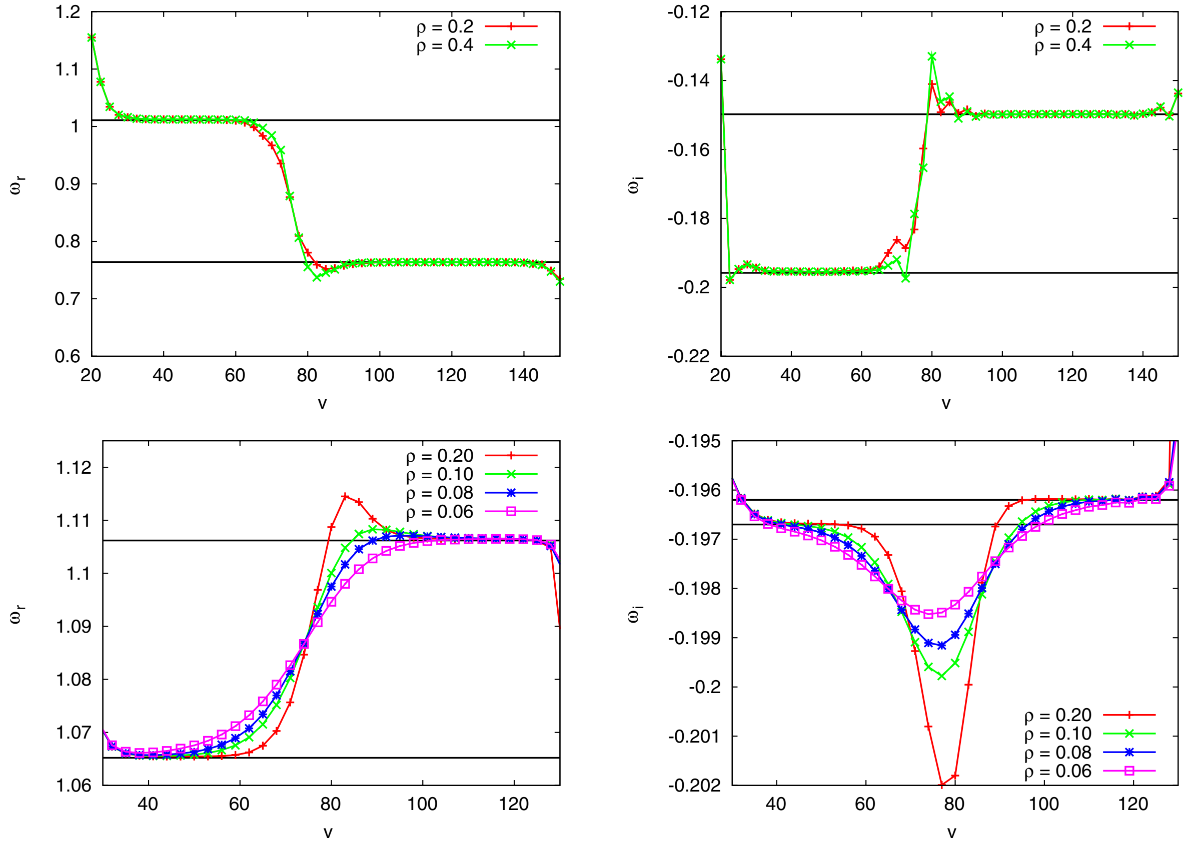

FIG. 2 (color online). (Top) ω_r (left) and ω_i (right) as function of v for the $\ell = 2$ scalar perturbation of a black hole with constant charge $q = 0.25$ and $m(v)$ given by (16) with $m_i = 0.5$, $m_f = 0.65$, $v_m = 75$ and different values of ρ_m. (Bottom) ω_r (left) and ω_i (right) as function of v for the $\ell = 2$ scalar perturbation of a black hole with constant mass $m = 0.5$ and $q(v)$ given by (16) with $q_i = 0.35$, $q_f = 0.4$, $v_m = 75$ and different values of ρ_q. In all graphics, the horizontal lines show the frequency values for static RN black holes with the initial and final configurations. The fit for the frequencies is typically more sensitive for the values of ω_i.

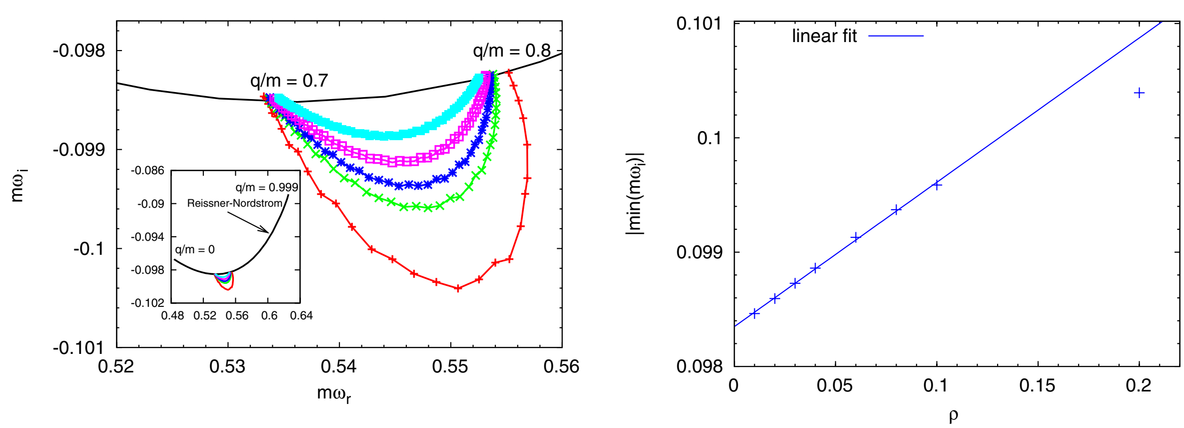

FIG. 3 (color online). (Left) $\omega_r \times \omega_i$ plane, showing the transition between equilibrium states for a varying charge case according to (16). The values of ρ_q for these curves are 0.04, 0.06, 0.08, 0.1, and 0.2 (from top to bottom). (Right) Minima of ω_i obtained in the transition shown in the left plot for different values of ρ_q, to quantify the nonadiabatic behavior.

We apply our numerical setup to simulate a charged black hole losing mass while keeping its charge constant, leading to a Reissner-Nordström naked singularity. For a fixed charge value q, we set a mass function (16) between two values m_i and m_f, and take the final mass to be $m_f < q$. At the point v_* when $m(v_*) = q$ the evaluation of $\varphi(u, v_*)$ is problematic since for the case of a naked singularity the full range of u must include the singularity

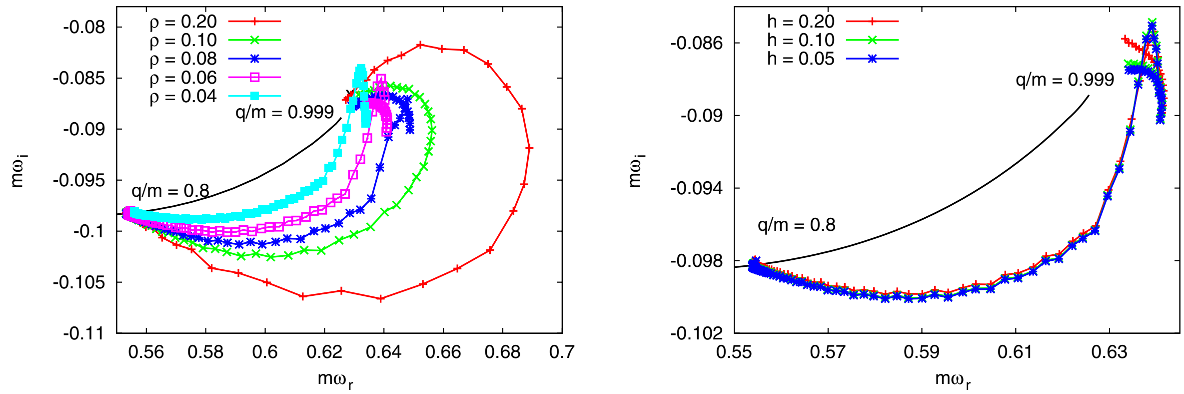

FIG. 4 (color online). (Left) $\omega_r \times \omega_i$ plane, showing the transition between equilibrium states for a varying charge case according to (16). The final state is an extremal RN black hole ($q = m$) and the values of ρ_q are the same as Fig. 3. (Right) Convergence test made for a fixed value of $\rho_q = 0.04$ and three different resolutions obtained with varying values for the integration stepsize h.

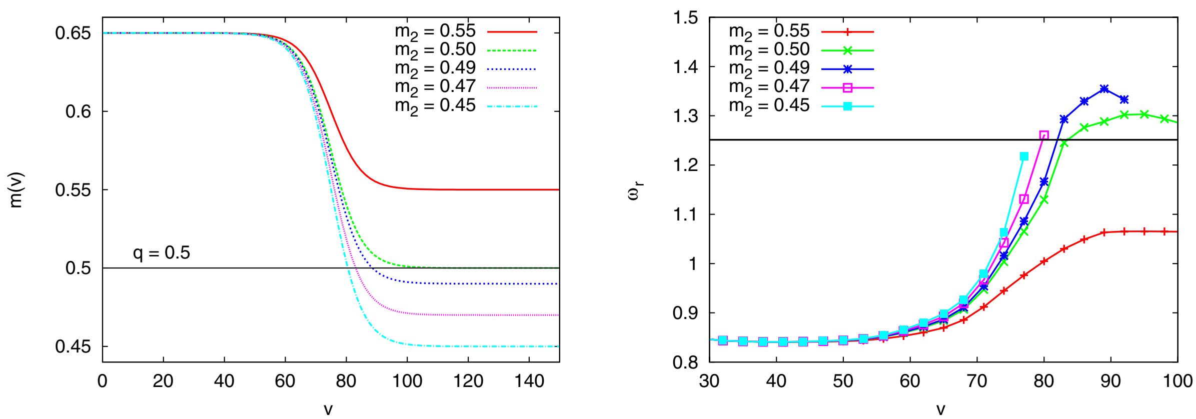

FIG. 5 (color online). (Left) Mass functions of the form (16) with $m_i = 0.65$, $\rho_m = 0.1$, $v_m = 75$ and different values of m_j, used to force the formation of a naked singularity while keeping $q = 0.5$ constant. (Right) ω_r as function of v for the $\ell = 2$ scalar perturbation of black holes with constant charge and varying masses as given in the left plot. The horizontal line shows the approximate frequency for an extremal RN black hole. The behavior of ω_i is quite similar but typically known with less precision.

at $r = 0$. Despite the fact that the scalar field can indeed be finite at $r = 0$ [44], our code cannot deal properly with the terms like $V(u, v)\varphi(u, v)$ in the vicinity of the singularity. This point is now under investigation, and a better numerical code is being developed for this case.

Our objective here is to investigate how the QNM behave until the very last moment before the formation of a naked singularity. The results obtained for the ω_r part of the QNMs are presented in Fig. 5. All simulations end at the point when an extremal RN black hole is formed, but the frequencies are all different. This is the result of the different nonstationary trajectories followed by the QNM in each case. We remark here that in the cases with a more rapid variation $m'(v_*)$ it seems there is not enough time before the simulation stops to see the maximum deviation of the frequency and the subsequent relaxation to a possible asymptotic value.

IV. FINAL REMARKS

Our results confirm, for the general Vaidya case, the same nonstationary behavior corresponding to the inertia of the QNM frequencies identified in [11]. In particular, for situations with $r''_+(v) > \omega_i(v)$, the QNM frequencies will not follow in the $\omega_r \times \omega_i$ plane a trajectory corresponding to the instantaneous frequency associated with an RN black hole of a given q/m ratio (see Figs. 3 and 4), and the inertial behavior of the QNM can be identified. Moreover, we see that the faster the change in $m(v)$ or $q(v)$ is, the bigger the deviation from the stationary regime will be. We could determine that the deviation from the stationary behavior is proportional to ρ for masses and charges varying according to (16), at least for values of $\rho \lesssim 0.1$; see Fig. 3.

Similarly to the uncharged case [11], the imaginary parts of the QNM frequencies are typically more sensitive to mass and charge changes than the real parts. However, we have identified a new behavior whose physical origin is still unclear for us: the QNM frequencies are typically more sensitive to charge than mass variations (compare the upper and lower graphics in Fig. 2).

This leads to a curious fact and a further conclusion. Consider two situations such that, in the first, electric charge is constant and mass is increasing, let us say according to (16). In the second, mass is constant and electric charge is varying in a way that both cases have the same quotient q/m as function of v. For these two situations, the instantaneous QNM frequencies will evolve differently in the $\omega_r \times \omega_i$. According to our results, the case of varying charge will typically show a bigger deviation from the stationary curve q/m. This new behavior demonstrates explicitly that the ratio q/m is not enough to characterize a nonstationary black hole. (This does not represent any challenge to the no-hair theorems, though, since they typically deal with stationary solutions.)

As for the $q = 0$ case considered in [11], an interesting extension of this work would be analysis of the highly damped QNM. Since for such overtones the ratio $|\omega_i/\omega_r|$ is always larger than for the fundamental ($n = 0$) QNM considered here, including, for sufficient large n, cases for which $|\omega_i/\omega_r| > 1$, it would be interesting to check if the stationary behavior could be improved for $n > 0$. In particular, it would be very interesting to test the high sensitivity of the instantaneous QNM overtones to electric charge variations. We remark that the numerical analysis presented here cannot be directly extended to the $n > 0$ case since one cannot identify the overtones numerically with sufficient accuracy. We believe, however, this could be attained by means of the WKB approximation.

ACKNOWLEDGMENTS

This work was supported by CNPq, FAPESP and the Max Planck Society. It is a pleasure to thank Rodrigo Panosso Macedo and Luciano Rezzolla for useful discussions.

[1] E. Berti, V. Cardoso, and A. O. Starinets, Classical Quantum Gravity **26**, 163001 (2009).
[2] R. A. Konoplya and A. Zhidenko, Rev. Mod. Phys. **83**, 793 (2011).
[3] E. Berti, V. Cardoso, and C. M. Will, Phys. Rev. D **73**, 064030 (2006).
[4] P. R. Brady, C. M. Chambers, W. Krivan, and P. Laguna, Phys. Rev. D **55**, 7538 (1997); P. R. Brady, C. M. Chambers, W. G. Laarakkers, and E. Poisson, Phys. Rev. D **60**, 064003 (1999).
[5] C. Molina, D. Giugno, E. Abdalla, and A. Saa, Phys. Rev. D **69**, 104013 (2004).
[6] D. P. Du, B. Wang, and R. K. Su, Phys. Rev. D **70**, 064024 (2004); E. Abdalla, B. Wang, A. Lima-Santos, and W. G. Qiu, Phys. Lett. B **538**, 435 (2002); E. Abdalla, K. H. C. Castello-Branco, and A. Lima-Santos, Phys. Rev. D **66**, 104018 (2002).
[7] R. A. Konoplya and A. Zhidenko, Nucl. Phys. **B777**, 182 (2007).
[8] S. Hod, Phys. Rev. D **66**, 024001 (2002).
[9] L. H. Xue, Z. X. Shen, B. Wang, and R. K. Su, Mod. Phys. Lett. A **19**, 239 (2004).
[10] C. G. Shao, B. Wang, E. Abdalla, and R. K. Su, Phys. Rev. D **71**, 044003 (2005).
[11] E. Abdalla, C. B. M. H. Chirenti, and A. Saa, Phys. Rev. D **74**, 084029 (2006).
[12] E. Abdalla, C. B. M. H. Chirenti, and A. Saa, J. High Energy Phys. 10 (2007) 086.
[13] X. He, B. Wang, S. F. Wu, and C. Y. Lin, Phys. Lett. B **673**, 156 (2009).
[14] B. Cuadros-Melgar and C. E. Pellicer, Phys. Rev. D **77**, 104030 (2008).
[15] B. Wang, Braz. J. Phys. **35**, 1029 (2005).
[16] H. Stephani *et al.*, *Exact Solutions of Einstein's Field Equations* (Cambridge University Press, Cambridge, England, 2002), 2nd ed.
[17] P. S. Joshi, *Global Aspects in Gravitation and Cosmology* (Oxford University Press, New York, 1993).
[18] K. Lake, Phys. Rev. Lett. **68**, 3129 (1992).
[19] J. P. S. Lemos, Phys. Rev. Lett. **68**, 1447 (1992); C. Hellaby, Phys. Rev. D **49**, 6484 (1994).
[20] D. M. Eardley and L. Smarr, Phys. Rev. D **19**, 2239 (1979).
[21] Y. Kuroda, Prog. Theor. Phys. **72**, 63 (1984).
[22] K. Lake and T. Zannias, Phys. Rev. D **41**, 3866 (1990).
[23] K. Lake and T. Zannias, Phys. Rev. D **43**, 1798 (1991).
[24] W. A. Hiscock, Phys. Rev. D **23**, 2813 (1981).
[25] Y. Kuroda, Prog. Theor. Phys. **71**, 100 (1984); **71**, 1422 (1984).
[26] W. Biernacki, Phys. Rev. D **41**, 1356 (1990).
[27] R. Parentani, Phys. Rev. D **63**, 041503(R) (2001).
[28] B.-L. Hu and E. Verdaguer, Living Rev. Relativity **7**, 3 (2004).
[29] A. B. Nielsen, M. Jasiulek, B. Krishnan, and E. Schnetter, Phys. Rev. D **83**, 124022 (2011).
[30] K. D. Krori and J. Barua J, J. Phys. A **7**, 2125 (1974).
[31] S. Chatterjee, B. Bhui, and A. Banerjee, J. Math. Phys. (N.Y.) **31**, 2208 (1990).
[32] A. Ori A, Classical Quantum Gravity **8**, 1559 (1991).
[33] F. Fayos, M. M. Martin-Prats, and J. M. M. Senovilla, Classical Quantum Gravity **12**, 2565 (1995).

[34] M. K. Parikh and F. Wilczek, Phys. Lett. B **449**, 24 (1999).
[35] A. Ishibashi and A. Hosoya, Phys. Rev. D **60**, 104028 (1999).
[36] B. R. Iyer and C. V. Vishveshwara, Pramana **32**, 749 (1989).
[37] S. G. Ghosh and N. Dadhich, Phys. Rev. D **64**, 047501 (2001); **65**, 127502 (2002).
[38] C. Chirenti and A. Saa, arXiv:1012.5110.
[39] F. Girotto and A. Saa, Phys. Rev. D **70**, 084014 (2004).
[40] A. Saa, Phys. Rev. D **75**, 124019 (2007).
[41] R. A. Konoplya, Phys. Rev. D **68**, 124017 (2003).
[42] V. D. Sandberg, Phys. Rev. D **12**, 2226 (1975).
[43] G. W. Gibbons, Commun. Math. Phys. **45**, 191 (1975).
[44] M. Martellini, C. Reina, and A. Treves, Phys. Rev. D **17**, 2573 (1978).
[45] F. Belgiorno, Phys. Rev. D **58**, 084017 (1998); D. Batic, D. Chin, and M. Nowakowski, Eur. Phys. J. C **71**, 1624 (2011).
[46] J. P. M. Pitelli and P. S. Letelier, Phys. Rev. D **77**, 124030 (2008).
[47] J. P. M. Pitelli and P. S. Letelier, Phys. Rev. D **80**, 104035 (2009).
[48] P. S. Letelier and J. P. M. Pitelli, Phys. Rev. D **82**, 043514 (2010).
[49] P. S. Letelier and J. P. M. Pitelli, Phys. Rev. D **82**, 104046 (2010).
[50] R. A. Konoplya, Phys. Rev. D **66**, 084007 (2002).